Damage to Spacecraft by Meteoroids and Orbital Debris

24.1 Introduction

Millions of meteoroids orbit around the sun and cross the orbit of the Earth around the sun.

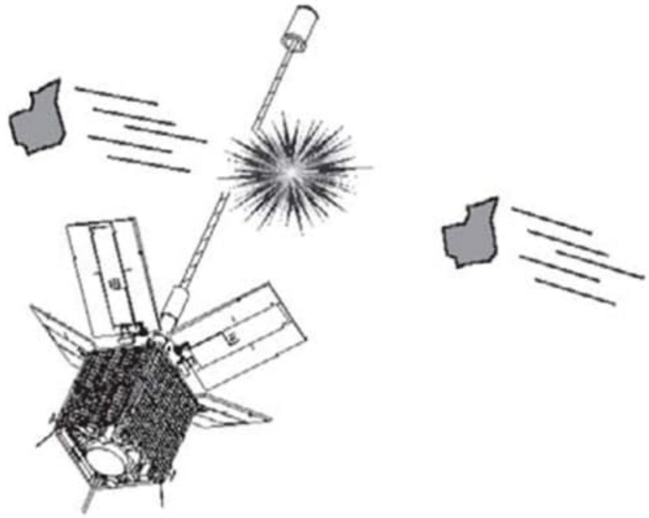

Fig. 24.1 Space debris collision with CERISE micro satellite stabilisation boom at 14 km/s in LEO (Courtesy SSTL)

Surrey Satellite Technology Ltd (SSTL) manufactured the CERISE micro satellite for Alcatel Espace (France) and the French MoD to carry out broad band radiometric measurements. CERISE was launched by Ariane in July 1995.

Many aspects about meteoroids and orbital debris environmental conditions and counter measures are discussed [IADC 2004].

24.2 Micro-Meteoroids and Space Debris Environment

The flux of particles for micro meteoroids and orbital debris are given in terms of the integral flux, which is the number of particles per m^2 per year of mass larger than or equal to m or diameter equal to or larger than d, impacting a randomly-orientated flat plate under a viewing angle of 2π radians.

24.2.1 Micro-Meteoroids Environment

The flux of micro-meteoroids (MM) is not constant but varies through the years. This is due to the micro-meteoroid showers (see Table 24.1). This happens if the orbit of the Earth crosses the orbits of the comets.

Table 24.1 Meteor showers [Tribble 2003]

Name	Date
Quantrantids	January 1–6
Lyrids	April 19–24
Eta Aquarids	May 2–7
Delta Aquarids	July 15–August 15
Perseids	July 27–August 17
Orionids	October 12–16
Taurids	October 26–November 25
Leonids	November 15–19
Geminids	December 7–14

Spacecraft have mission durations varying from some weeks to several years, therefore the mean flux of the MMs is sufficient to analyse the effects of MM's on spacecraft. The interplanetary flux of MM can be defined with the following Gruens formula [Drolshagen 1992, Tribble 2003]

$$F_{MM} = c_0\{F_1(m) + F_2(m) + F_3(m)\}\ \mathrm{m^{-2}/year} \tag{24.1}$$

where

$$F_1(m) = (c_1 m^{0.306} + c_2)^{-4.38}$$

$$F_2(m) = c_3(m + c_4 m^2 + c_5 m^4)^{-0.36}$$

$$F_3(m) = c_6(m + c_7 m^2)^{-0.85}$$

$$c_0 = 3.15576\times10^7,\ c_1 = 2.2\times10^3,\ c_2 = 15,\ c_3 = 1.3\times10^{-9},$$

$$c_4 = 1\times10^{11},\ c_5 = 1\times10^{27},\ c_6 = 1.3\times10^{-16}\ \text{and}\ c_7 = 1\times10^6$$

The function F_1 refers to large particles ($m > 1\times10^{-9}$ g), function F_2 to intermediate-sized particles ($1\times10^{-14} \le m \le 1\times10^{-9}$ g) and function F_3 to small particles ($m \le 1\times10^{-14}$ g).

The average velocity of the MM particles is about 17 km/s. The velocity ranges from 11 to 72 km/s. The NASA 90 velocity density is analytically defined by

$$f(v) = \begin{cases} 0.112 & \text{if } 11.1 \le v \le 16.3 \text{ km/s} \\ 3.328\times10^{5} v^{-5.34} & \text{if } 16.3 \le v \le 55 \text{ km/s} \\ 1.695\times10^{-4} & \text{if } 16.3 \le v \le 72.2 \text{ km/s} \end{cases} \quad (24.2)$$

The MM flux F_{MM} shall be corrected to account for Earth shielding. The correction parameter $\xi(h)$ is given by

$$\xi_{\mathrm{mean}}(h) = \frac{1+\cos\theta}{2}, \quad (24.3)$$

where h (km) is the height of the orbit and the angle θ is defined as

$$\sin\theta = \frac{R_{\mathrm{E}}+100}{R_{\mathrm{E}}+h}, \quad (24.4)$$

with R_{E} the mean radius of the Earth (6378 km) and $h \ge 100$ km.

Due to the gravitational field of the Earth, meteoroid particles are attracted and the flux increases compared with deep space. This effect is taken into account by the defocusing factor G_{E}, that is

$$G_{\mathrm{E}} = 1 + \frac{R_{\mathrm{E}}+100}{R_{\mathrm{E}}+h}. \quad (24.5)$$

For planes pointing to Earth the MM flux will be reduced with a factor of 10. The reduction factor F_{dir} is defined by

$$F_{\mathrm{dir}}(h) = \frac{1.8+3\sqrt{1-\left(\frac{R_{\mathrm{E}}+100}{R_{\mathrm{E}}+h}\right)^2}}{4} \quad (24.6)$$

Considering the Earth shielding, the gravitational defocussing and the direction reduction factor will lead to a particle flux

$$F_{\mathrm{C}}(m,h) = F_{\mathrm{MM}}(m)G_{\mathrm{E}}(h)\xi_{\mathrm{mean}}(h)F_{\mathrm{dir}}(h)$$

24.2.2 Orbital debris Environment

The orbital debris (OD) is encountered in orbits around the Earth with an approximate velocity 8 km/s. The OD is dependent on the diameter d (cm) of the OD particle and is given in a number of OD particles per year and per m^2

$$F_{OD} = H(d)\Phi(h,S)\Psi(i)[F_1(d)g_1(t) + F_2(d)g_2(t)] \tag{24.8}$$

where

$H(d) = \sqrt{\left[10^{e^{-\left(\frac{\log d - 0.78}{0.637}\right)^2}}\right]}$, this function is called the Henize function

$$H(x,y) = \sqrt{10^{e^{-\frac{x^2}{y}}}}$$

$$\Phi(h,S) = \frac{\Phi_1(h,S)}{\Phi_1(h,S)+1}, \text{ and } \Phi_1(h,S) = 10^{\left(\frac{h}{200} - \frac{S}{140} - 1.5\right)}$$

$$F_1(d) = 1.22\times10^{-5}d^{-2.5}, \text{ and } F_2(d) = (8.1\times10^{10})(d+700)^{-6}$$

$$g_1(t) = (1+q)^{(t-1988)}, \text{ and } g_2(t) = 1 + p(t-1988)$$

The height is $h < 2000$ (km), the angle of orbital inclination i is in degrees, the time t is n years with $t \le 2011$. The assumed growth rate of intact objects is $p \approx 0.05$ and the estimated growth rate of fragments is $q \approx 0.02$.

The function $\Psi(i)$ gives the relation between the orbital inclination and the OB flux.

The function is given in the following Table 24.2.

Table 24.2 Inclination dependent function $\Psi(i)$

Inclination i (degrees)	$\Psi(i)$
up to 28.5	0.91
30	0.92
40	0.96
50	1.02
60	1.09
70	1.26
80	1.71
90	1.37
100	1.78
120	1.18
up to 360	1.18

S, the 13-month smoothed solar radio flux with a wave length of 10.7 cm ($F_{10.7}$) for year $t-1$, is expressed in 1×10^4 J. A typical value of the solar radio flux is $S = 100$.

The solar radio flux $F_{10.7}$ is given in Table 24.3.

Table 24.3 $F_{10.7}$ in year $t-1$

Year	$F_{10.7}$ in year $t-1$	Year	$F_{10.7}$ in year $t-1$
2005	118	2014	180
2006	80	2015	137
2007	76	2016	118
2008	74	2017	80
2009	75	2018	76
2010	106	2019	74
2011	163	2020	75
2012	198	2021	106
2013	190	2022	163

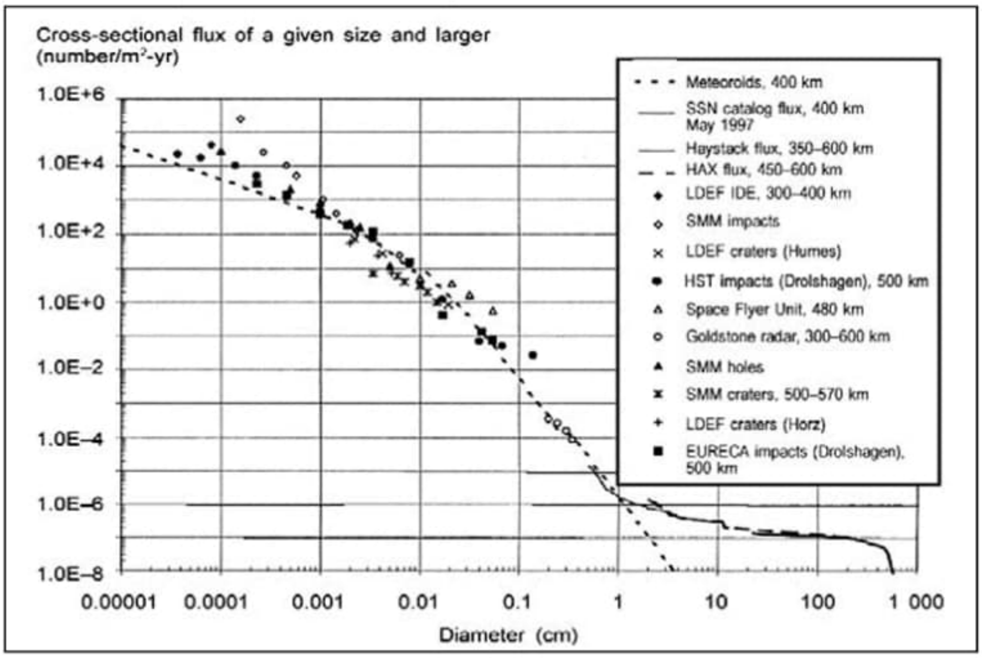

Fig. 24.2 Approximate measured debris flux in low Earth orbit, by object size [ISIS 2000]

For bodies in LEO, whether orbital debris or spacecraft, there is only a small change in speed versus altitude even out to 2000 km, and the average speed is about 7.7 km/s (at 500 km). However, because different objects are in different orbits, collisions are possible between 0–15.4 km/s, with an average speed of about 10 km/s.

Fig. 24.2 presents a compilation of the results of many of the measurement systems described in previous sections. It shows the cross-sectional flux (number of objects per year per square metre) for objects of a given size and larger. The figure summarizes measurements in LEO near an altitude of 500 km.

The development of MOD protection systems allows the designers to reduce the risk of spacecraft failure. Risk may be defined as the probability of critical failure or loss of spacecraft, or simply the probability of any spacecraft malfunction. The decision to protect a spacecraft is governed by the compromise between accepting a reasonable level of risk, and the cost of implementing protection methods. A flowchart which illustrates the general algorithm involved in the development of MOD threat assessment is shown in Fig. 24.3.

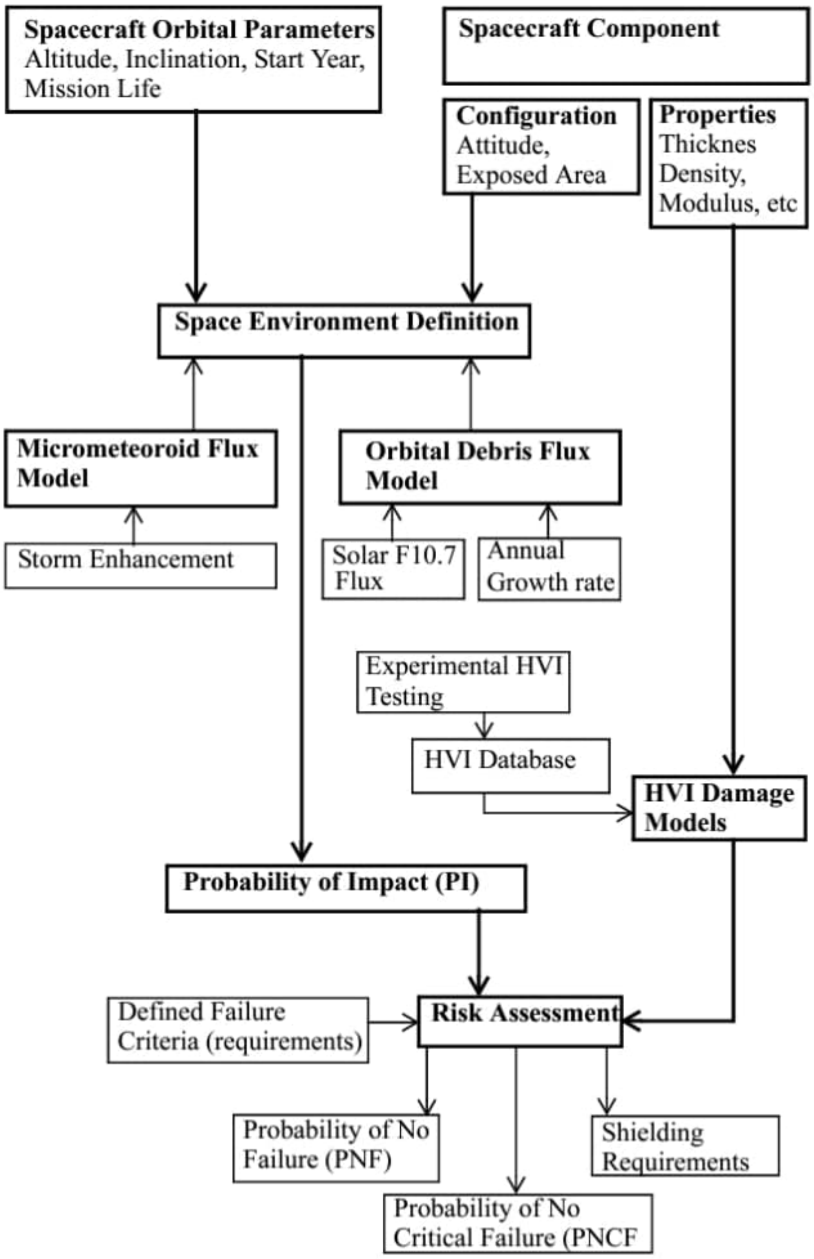

Fig. 24.3 MOD threat assessment flowchart

24.3 Hyper Velocity Impact Damage Models

Many impact damage models are discussed in [Elfer 1996, IADC 2004].

24.3.1 Single Plate Penetration Equations

The following equation was developed by Fish and Summers [Hayashida 1991]. They used test results with velocities which ranged from 0.5–8.5 km/s, metallic targets which ranged in density from magnesium-lithium alloy to beryllium-copper alloy, and with aluminium alloy. The velocity vector is perpendicular to the plate. This equation was recommended for design to establish the threshold penetration (ballistic limit) of thin, ductile, metal plates.

$$t = K_1 m_p^{0.352} v_p^{0.875} \rho_p^{\frac{1}{6}}, \qquad (24.9)$$

where t is the target thickness (cm), m_p is the projectile mass (gr), v_p is the impact velocity (km/s), ρ_p is the projectile density (gr/cm^3) and K_1 is a constant $K_1 = 0.57$ for Al-alloys such as 2024-T3, 2024-T4, 6061-T6 and 7075-T6. $K_1 = 0.70$ was used to determine the plate thickness to prevent penetration from spalling (spallation limit).

The mass density ρ_p (gr/cm^3) of the projectile is discussed in [Drolshagen 1992] and can be obtained by the following equation

$$\rho_p(d) = \frac{2.8}{d^{0.74}}, \qquad (24.10)$$

where the projectile diameter d is in (cm).

If a spherical particle is assumed, the mass m_p (gr) can be expressed in the density ρ_p (gr/cm^3) and the diameter d_p (cm)

$$m = \frac{1}{6}\pi\rho d^3. \qquad (24.11)$$

The cratering or depth of penetration p (cm) in a single wall is given by [Elfer 1996]

$$p = K_i m_p^{0.352} v_p^{0.667} \rho_p^{\frac{1}{6}}, \qquad (24.12)$$

where $K_1 = 0.42$ for Al-alloys and $K_1 = 0.25$ for 304 and 316 stainless steel.

The entry crater diameter D_c (mm) for composite materials in space is given by [Tennyson 1997]

$$D_c = 1.05\sqrt[3]{\frac{E_{\text{kin}} t \rho_t}{D_p \rho_p}}. \tag{24.13}$$

where E_{kin} the kinetic energy of the projectile (J), $E_{\text{kin}} = \frac{1}{2} m_p v_p^2$, D_p diameter of projectile (mm), ρ_t and ρ_p are the target and projectile densities and t the target thickness (mm).

The model is applicable to PEEK and epoxy matrix based composites. The carbon fibres used all have a modulus in between 135–235 GPa. Applicable laminate thicknesses range from 0.5–6.7 mm. The model is independent of the laminate lay-up. The model is consistent for a broad band of projectile diameters, extending from 0.4–9.13 mm, travelling at velocities ranging from 4–7.5 km/s. Al-alloy, glass, nylon and steel projectiles are compatible with the model.

24.3.2 Multi-shock shield

The **Whipple Shield** is the first spacecraft shield ever implemented. It was introduced by Fred Whipple back in the 1940s, and is still in use today. Basically, it consists of placing a sacrificial bumper, usually aluminium, in front of the spacecraft, thus allowing it to absorb the initial impact. The Whipple bumper shocks the projectile and creates a debris cloud containing smaller, less lethal, bumper and projectile fragments. The full force of the debris cloud is diluted over a larger area on the spacecraft rear wall. The Whipple shield is illustrated in Fig. 24.4.

The **Stuffed Whipple Shield** is a variation of the simple Whipple shield. Layers of Nextel and Kevlar are inserted in between the bumper and the rear wall. These additional layers further shock and pulverize the debris cloud such that any fragments reaching the rear wall are benign.

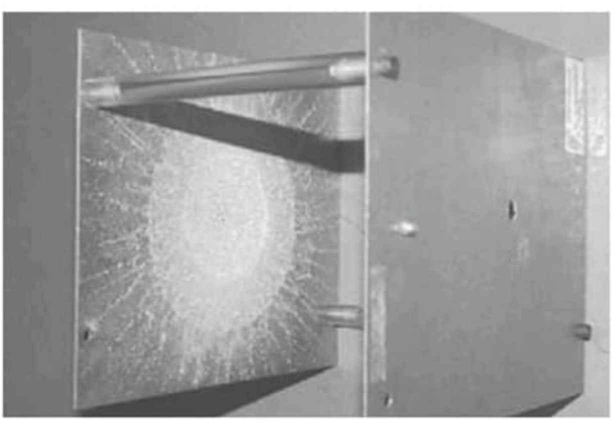

Fig. 24.4 Whipple Shield [hitf.jsc.nasa.gov]

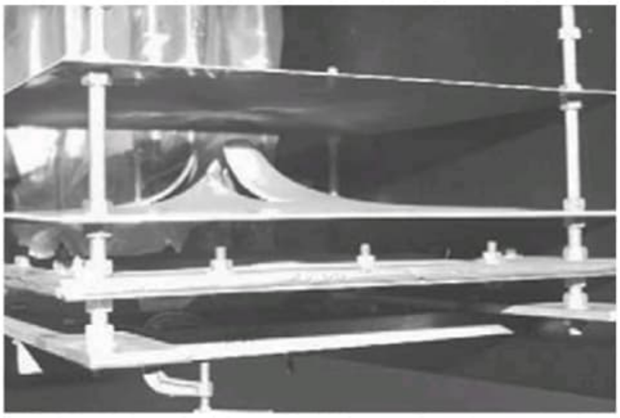

Fig. 24.5 Stuffed Whipple Shield

In this section only the equations for the whipple shield are given. The equations for other type of shield can be found in [Elfer 1996].

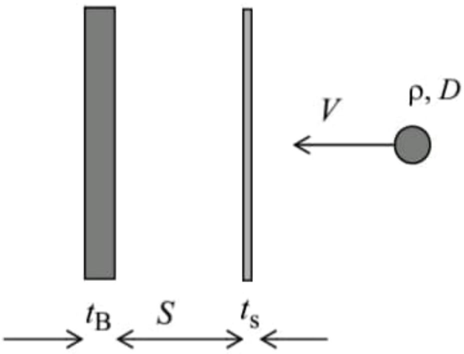

Fig. 24.6 Whipple shield

Examples from the International Space Station (ISS) [NRS 1997]. These applications are shown in Fig. 24.7.

Whipple Shield

The distance between the rear wall is in general $S \geq 15D$ and the thickness of the bumper shield

$$t_b = \frac{c_b m_p}{\rho_b} = \frac{c_b D \rho_p}{\rho_b}, \tag{24.14}$$

where t_b is the thickness of the bumper shield (cm), m_p is the mass of the particle (gr), ρ_b is the density of the bumper material (g/cm^3) and ρ_p is the density of the particle (g/cm^3). The constant c_b depends upon the ratio of the distance S and the particle diameter D.

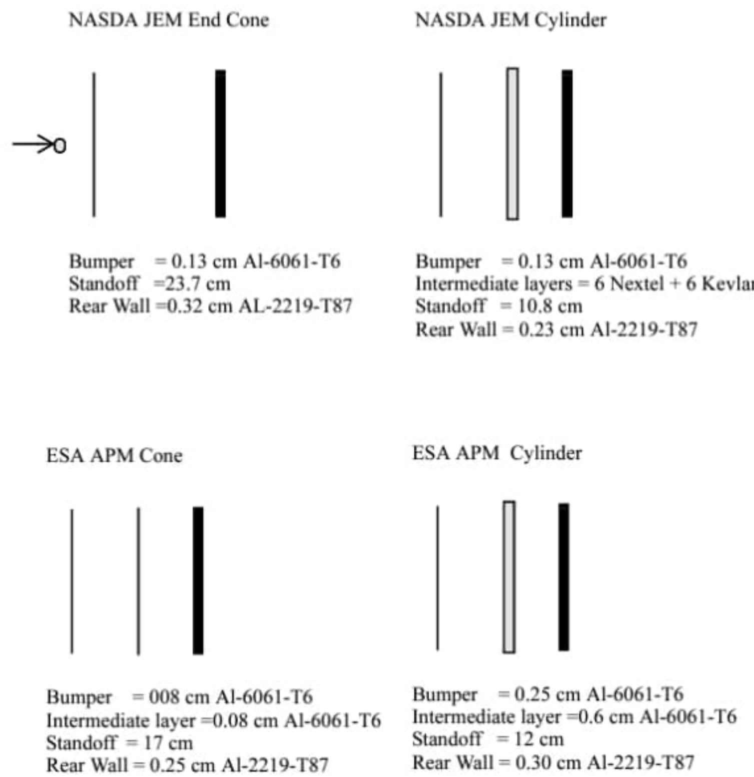

Fig. 24.7 Examples ISS shield configurations [NRC 1997]

$$c_b = \begin{cases} 0.25 & \frac{S}{D} < 30 \\ 0.20 & \frac{S}{D} \geq 30 \end{cases} \tag{24.15}$$

The thickness of the rear wall t_w, to prevent spall detachment, can be calculated [Drolhagen 1992]

$$t_w = c_w(\rho_p \rho_b)^{\frac{1}{6}} m_p^{\frac{1}{3}} \frac{V}{\sqrt{S}} \sqrt{\frac{70}{\sigma_y}} \tag{24.16}$$

where

- t_w is the threshold rear wall sheet thickness (cm)
- ρ_b is the rear wall material density (g/cm^3)
- ρ_p is the projectile density (g/cm^3)
- S the spacing between shield and rear wall
- V the speed of the projectile $6<V<9.8$ km/s
- σ_y the yield stress in (ksi)

Equations for multi shock shield can be found in the literature, especially in [Elfer 1996].

24.4 Probability of Impacts

The probability that k meteoroids or particles of orbital debris will have a collision with a spacecraft can be estimated with Poisson (Simeon-Denis Poisson 1781–1840) probability density function

$$p_k = e^{-\lambda}\frac{\lambda^k}{k!},\ k = 0, 1, \ldots . \tag{24.17}$$

The probability density function of Poisson is illustrated in Fig. 24.8.

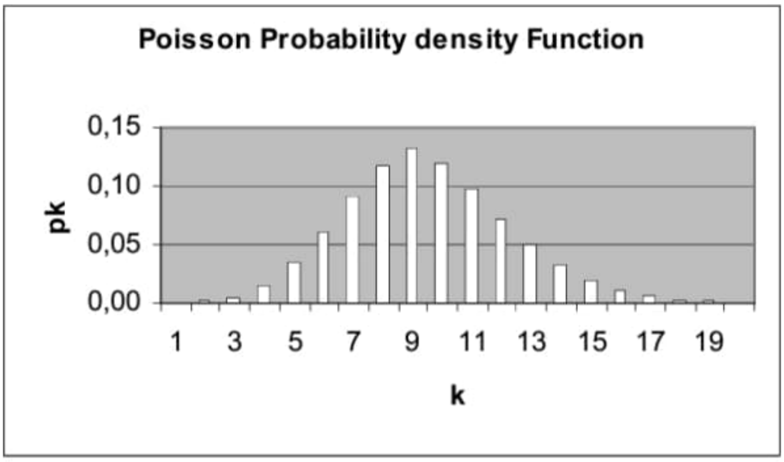

Fig. 24.8 Poisson Probability Density Function, $\lambda = 9$

If a stochastic variable X indicates the total number of successes in case of a large number of independent executions of an experiment with a very little probability of success, then the probability can be approximated by

$$P(X{=}k) = e^{-\lambda}\frac{\lambda^k}{k!}, \tag{24.18}$$

for which the value for λ is the product of the number of experiments and the probability of success.

The probability $P(X \le k)$ is given by

$$P(X \le k) = e^{-\lambda}\left(1 + \frac{\lambda}{1!} + \frac{\lambda^2}{2!} + \ldots + \frac{\lambda^k}{k!}\right), \tag{24.19}$$

thus

$$P(X \leq \infty) = 1 \tag{24.20}$$

The average or expected value $E(X) = \mu_X = \lambda$ and the variance $\sigma_X^2 = \lambda$.
The probability of no impact (PNI) $P(k=0)$, or no collisions is given by

$$P(k=0) = e^{-\lambda} \tag{24.21}$$

where the total number of impacts, or fluence λ, a spacecraft can expect to experience is the product of the flux F (number of particles per year per m2), the spacecraft's exposed area A (m^2) and the mission duration T_M (years). The relationship is expressed as

$$\lambda = FAT_M \text{ (particles).} \tag{24.22}$$

The probability of impact (PI), at least one impact is expressed as the complement of the PNI (see (24.19))

$$P(k=1) = 1 - e^{-\lambda}, \tag{24.23}$$

where $F(x)$ is given by (24.1) and (24.8) or Fig. 24.2.